Published in final edited form as:
*Langmuir*. 2009 January 6; 25(1): 568–573. doi:10.1021/la802728p.

# Ion Channel Mimetic Chronopotentiometric Polymeric Membrane Ion Sensor for Surface Confined Protein Detection

**Yida Xu**[a] and **Eric Bakker**[b]

a*Department of Chemistry, Purdue University, IN 47907, USA*

b*Nanochemistry Research Institute, Department of Applied Chemistry, Curtin University of Technology, Perth, WA 6485, Australia*

## Abstract

The operation of ion channel sensors is mimicked with functionalized polymeric membrane electrodes, using a surface confined affinity reaction to impede the electrochemically imposed ion transfer kinetics of a marker ion. A membrane surface biotinylated by covalent attachment to the polymeric backbone is used here to bind to the protein avidin as a model system. The results indicate that the protein accumulates on the ion-selective membrane surface, partially blocking the current induced ion transfer across the membrane/aqueous sample interface, and subsequently decreases the potential jump in the so-called super-Nernstian step that is characteristic of a surface depletion of the marker ion. The findings suggest that such a potential drop could be utilized to measure the concentration of protein in the sample. Because the sensitivity of protein sensing is dependent on the effective blocking of the active surface area, it can be improved with a hydrophilic nanopore membrane applied on top of the biotinylated ion-selective membrane surface. Based on cyclic voltammetry characterization, the nanoporous membrane electrodes can indeed be understood as a recessed nanoelectrode array. The results show that the measuring range for protein sensing on nanopore electrodes is shifted to lower concentrations by more than one order of magnitude, which is explained with the reduction of surface area by the nanopore membrane and the related more effective hemispherical diffusion pattern.

## Introduction

Electrochemical affinity biosensors typically require an amplification step in order to reach attractive detection limits. This is typicallynormally accomplished by coupling the biochemical recognition step to a catalytic amplification with enzyme labels,[1] the dissolution of nanoparticles[2, 3] or liposome labels,[4, 5] similarly yielding a multitude of detectable species for each binding event. Ion-channel mimetic sensors represent another direction to yield a chemical amplification step, and are especially suited for surface confined binding events. Different types of ion-channel sensors have been developed, and pioneering work in this direction was performed on metal electrodes or carbon electrodes, typically with a redox marker present in the sample whose access to the electrode surface was hindered by a target molecule induced binding process at that surface,[6–9] which makes it possible to gain information on the concentration of the target compound in an indirect, amplified manner. As the name implies, this mimics the processes that occur at natural ion channel proteins.

Recent research has also focused on liquid–liquid or liquid-polymeric interfaces, since these appear to be more representative of ion channel mimetic materials found in biological systems.

Correspondence to: Eric Bakker.

Similar to natural ion channel proteins, the marker species in these cases are not redox active, but sample ions for which the membrane is selective.[10, 11]

One early example includes the ion transfer at the interface of two immiscible electrolytes (ITIES) coated with layers of surfactants or phospholipids, altering the observed ion transfer current–voltage characteristics.[12, 13] In other work, chemically modified ion channels were fabricated to allow for affinity biorecognition, in which case the modulated zero current ion flux across the ion channels was monitored with potentiometric sensors.[14] In a more direct approach, biosensing components with lipophilic surfactant-like properties were incorporated in ion-selective membranes. The resulting self-assembled layer at the sample/membrane interface was shown to alter the interfacial ion transport characteristics, and was predominantly investigated by electrochemical impedance spectroscopy.[15] In this case, the low frequency range of the Nyquist plot is was altered as a consequence of a biorecognition process.[15 16]

In this paper, a pulsed galvanostatic chronopotentiometric polymeric membrane ion sensor (so-called pulstrode) with biomaterial modified surface is investigated for surface affinity biosensing purposes. In this case, the binding event is expected to increase the energetics of the instrumentally imposed ion flux across the chemically modified sample–membrane interface. Early work with this general protocol has been performed on non-specific membrane coatings, including surfactants and polyelectrolyte layers.[17, 18] It was established that the technique is most sensitive to surface blocking events under conditions where a depletion of the marker ion in the aqueous phase boundary of the membrane is observed.[17, 19] This region is well characterized in the pulsed chronopotentiogram with the occurrence of a so-called super-Nernstian response slope.[19, 20] Related experiments using zero-current potentiometry to probe fluxes across biofunctionalized polyurethane membrane were met with only limited success, [21] likely because the ion fluxes were difficult to adjust with this passive technique. A more dynamic electrochemical approach such as the one utilized here is more beneficial to interrogate ion-channel mimetic membrane materials.

Any ion transfer blocking effect based sensing protocol is subject to the extent of the ion transport blockage, and a more sensitive measurement is expected if the effective area available for ion transfer is reduced. Track-etched nanoporous membranes commonly made of polycarbonate and poly(ethylene terephthalate) have been successfully explored for this purpose.[22] A heavy ion beam is used for membrane tracking and subsequent etching in concentrated hydroxide solution forms the desired pores. The pore diameter has been demonstrated to be linearly related to the etching time and the electrochemical monitoring of a single-sided etching process produces conically shaped pores.[23, 24] The characterization of nanopore membranes has been conducted by cyclic voltammetry, chronoamperometry and scanning electrochemical microscopy.[25–28] The presence of an affinity bioreagent can substantially block the ion transport and decrease the frequency of ion transfer.[24, 29]

## Experimental

### Reagents

Avidin (from egg white) was purchased from Sigma. (+)-Biotinyl-3, 6, 9-trioxaundecanediamine (Amine-Biotin-$PEO_3$) was obtained from Pierce. 1,2-Dipalmitoyl-*sn*-Glycero-3-phosphoethanolamine-N-Biotinyl sodium salt (biotin lipid) was from Avanti Lipids. High molecular weight poly(vinyl chloride) (PVC), poly(vinyl chloride) carboxylated (PVC-COOH, 1.8% carboxyl content), 2-nitrophenyloctyl ether (*o*-NPOE), tetradodecylammonium tetrakis-(4-chlorophenyl)borate (ETH 500), tetrahydrofuran (THF), sodium ionophore tert-butyl calix[4]arene tetraacetic acid tetraethylester (Na-X), 2-(N-morpholino)ethanesulfonic acid (MES) and all salts were purchased from Fluka Chemical Corp. (Milwaukee, WI). 1-ethyl-3-(3-dimethylaminopropyl) carbodiimide hydrochloride

(EDC) and Trishydroxymethylaminomethane (Tris) were provided by Acros and J. T. Baker, respectively. Calcium ionophore N, N-Dicyclohexyl-N'-phenyl-N'-3-(2-propenoyl)-oxyphenyl-3-oxapentanediamide (AU-1) was synthesized in our laboratory.[30] Aqueous solutions were prepared by dissolving the appropriate salts in Nanopure-deionized water (18.2 MΩ cm). The track-etched hydrophilic polycarbonate nanopore membranes (pore density $\rho = 4 \times 10^8$ pores/cm$^2$, average pore diameter 2r = 100 nm and film thickness L = 6 μm) wetted with poly(vinylpyrrolidone) (PVP) were obtained from Sterlitech Corporation.

## Biotin Modification

Two biotin derivatives were used in the two ways of biotin modification of the sensing membranes, respectively. One is (+)-Biotinyl-3, 6, 9-trioxaundecanediamine (Amine-Biotin-$PEO_3$), which was used in the biotin functional group covalent attachment to the membrane; the other is 1,2-Dipalmitoyl-*sn*-Glycero-3-phosphoethanolamine-N-Biotinyl sodium salt (biotin lipid), which was directly doped into the membrane matrix in the solvent casting process. For covalent attachment, first a regular sodium-selective or calcium-selective membrane was cast with THF cocktail containing 10 mmol/kg Na ionophore X or 20 mmol/kg Ca ionophore Au-1, 10 wt.% lipophilic salt ETH 500, 1:2 (weight ratio) PVC and *o*-NPOE in a glass ring fixed on a glass plate by rubber bands. After the membrane (total mass about 220 mg) was completely dry, 8.06 mg PVC-COOH dissolved in 0.5 mL THF was poured onto the membrane surface, yielding an approximately 7-μm thick PVC-COOH film on the basis of the relative membrane masses used. A two-layer membrane formed after evaporation of THF. Amine-Biotin-$PEO_3$ was linked to PVC-COOH surface by using the procedure as following: 2% EDC (in ethanol) solution was first used to activate surface for about 5 min. Second, the solution was discarded and a mixture of 40 μL 1.9 mM EDC, 250 μL 3 mM Amino-Biotin-$PEO_3$ and 1.5 mL 10 mM MES-NaOH buffer (pH = 5.36) were poured onto the membrane (EDC and Amino-Biotin-$PEO_3$ were also dissolved in the same MES buffer) and stirred for 2 h. Third, the membrane was washed with MES-NaOH buffer and air-dried. To dope the biotin lipid, a biotin layer was spin-coated on the regular ion-selective membrane surface by using 100 μL cocktail containing 0.29 mg biotin lipid, 0.31 mg Na ionophore X, 46.48 mg PVC, 97.82 mg *o*-NPOE and 1.5 g THF.

## Electrodes

The ion-selective membranes were cut with a cork borer (6-mm diameter) from the parent membrane and incorporated into Philips electrode bodies (IS-561, Glasbläserei Möller, Zürich, Switzerland). The inner solution consisted of 0.1 M NaCl and was contacted with an internal Ag/AgCl electrode. The electrodes were conditioned overnight before experiments in a solution identical to the inner filling solution. A double-junction Ag/AgCl electrode with 1 M LiOAc bridge electrolyte was used as an external reference electrode.

## Experimental Setup

Chronopotentiometry measurements were conducted in a three-electrode cell system where the Philips body electrode acted as a working electrode and the external reference electrode and counter electrode (platinum wire) were immersed into the sample. The pulsed galvanostatic/potentiostatic technique was utilized in the control of the ion-selective membrane, which was described in detail elsewhere.[20, 31] The chronopotentiometry experiments were performed with an AFCBP1 bipotentiostat (Pine Inst., Grove City, PA) controlled by a PCI-MIO-16E4 interface board and LabVIEW Software (National Instruments, Austin, TX) on a Macintosh computer. Prior to the experiment, the operation of the first electrode output of the bipotentiostat (K1) was switched to current control with potentiostatic control of output of second working electrode (K2). To apply the current pulse, the working electrode was connected to the K1 output via an analog switch controlled by external software.

When the baseline potential between current pulses was applied, the working electrode was connected to the K2 output. During the experiments, each applied constant current pulse (of 0.5-s duration) was followed by another constant zero current pulse (of 0.5-s duration), then a constant potential pulse (of 25-s duration) was added. Sampled potentials, which represented the sensor response, were obtained as the average value during the last 50 ms of each current pulse.

### Avidin assembly

Avidin was deposited onto the electrode membrane surface by immersing the membrane on the electrode in the avidin solution for 2 min under stirring and 10 min under non-stirring. Subsequently, the electrode surface was rinsed with the same buffer before electrochemical measurement. All solutions were buffered to pH 7.4 with 1 mM Tris-HCl buffer in 10 mM magnesium nitrate background.

### Electrochemical impedance spectroscopy measurement

All EIS studies were undertaken using a Princeton Applied Research Parstat 2273 instrument. Experimental control and data acquisition were performed by using a personal computer running the PowerSINE software. EIS spectra were collected when using A.C. amplitude of ±10°mV rms and a frequency range of 100kHz–100mHz.

### Cyclic voltammetry measurement

Cyclic Voltammetry measurements were conducted in a traditional three-electrode cell same as in chronopotentiometric experiments with CH 910 bipotentiostat (CH Instruments InC., Austin, TX) at ambient temperature. All samples contained 1 mM sodium chloride as background electrolyte.

## Results and Discussion

Chemical modification and biofunctionalization of ion-selective membranes were reported earlier for enzymatic sensors in order for the incorporated enzymes to produce the ions that could be sensitively detected by the membrane.[32] The direct immobilization of enzymes such as urease on ion-selective membranes was realized via chemical reaction of the amino acid units of the enzymes to either carboxylic or amine groups of the polymer membrane matrix or to activated cellulose triacetate with the assistance of carbodiimide or glutaraldehyde.[33–35] Here, we aimed at introducing biotinylated functionality on the polymeric membrane surface in order to selectively bind avidin from the sample. A first attempt explored the spontaneous assembly of a lipophilic biotin lipid layer on top of a chemically unmodified ion sensing membrane, which gave poorly reproducible results (data not shown). It was therefore decided to use a covalent binding approach, by reacting Amine-Biotin-$PEO_3$ and carboxylated PVC in the presence of EDC catalyst, anticipating that the PEO segments in the biotin ligand could help decrease the effect of non-specific adsorption. The second method was found to be more robust and stable and was utilized in the following experiments unless noted otherwise.

Figure 1 illustrates the impedance spectra of the sodium-selective electrodes with and without biotin functionalization on the membrane surface. After the membrane was treated with avidin solution, an increase in both the so-called Warburg impedance and phase shift were observed, no matter whether or not the membrane surface was modified with biotin ligand. This is in accordance with previous observations on ion-selective membranes that were coated by surfactants or polyelectrolytes.[17, 18] The difference between biotin modified and unmodified membranes can be clearly observed, however. First, the bulk membrane resistance before avidin reaction is larger for the biotinylated membrane, see the enlarged semicircle in the high frequency range of the Nyquist plot (see also [36]). Only two semicircles can be distinguished

in Figure 1, because the semicircles only represent the bulk membrane resistance if the ionic strength of aqueous solution is not very low. Here, the bigger semicircle denotes the experiments with biotin-modified membrane and the smaller semicircle signifies the experiments using membranes without biotin modification. Second, the impedance response to avidin is more significant for the biotinylated membrane. Third, the impedance response gradually decreased upon washing with buffer solution for unfunctionalized membranes, but was found to be very stable and independent of washing steps with the biotinylated surface. This is suggestive of the strong interaction between avidin and the biotin linked membrane.

Such difference can also be demonstrated in pulsed chronopotentiometric experiments. As shown in Figure 2, if the membrane is not modified with biotin, the potential change upon successive addition of sodium chloride to 10 mM magnesium nitrate (pH 7.4) does not exhibit a significant difference after the membrane is treated in avidin solution, suggesting a low coverage of the membrane surface by the protein molecules. In contrast, a much larger chronopotentiometric response is observed for the biotinylated membrane surface, see Figure 3. This suggests that the surface bound protein coverage is enhanced significantly via strong biotin-avidin interactions, which leads to a more effective blocking of the sodium ion flux across the sample/membrane interface.

In Figure 3, sodium chloride was successively added to the sample containing 10 mM magnesium nitrate at pH 7.4, and this experiment was repeated after the electrode membrane was treated with 1 mL of 0.18 mg/mL avidin solution (with the same buffer) for 12 min and subsequent rigorous buffer washing. The ion transfer blocking effect is most prominent in the so-called super-Nernstian concentration range around 1 mM sodium, which is indicative of sodium ion depletion in the vicinity of membrane surface induced by the cathodic current pulse. A two-layer sandwich membrane with a top layer doped with biotin lipid showed a similar effect (data not shown). Compared to the response of sodium-selective electrodes made up of unmodified membrane, the position of the super-Nernstian step from biotin functionalized membrane before avidin treatment shifted to higher sodium concentrations by about 1 order of magnitude,[17] probably because of the hindrance from the additional biotin layer.

Note, however, that not all ions could be applied as markers to monitor the protein blocking effect. When a calcium-selective membrane with a top layer incorporated with biotin lipid was utilized, the potential response to calcium ions did not significantly change upon protein exposure, even though all other parameters were kept same (data not shown). This may be explained by the possible interaction of calcium ions and the carboxyl groups in the protein, which may result in two competing effects: the surface coverage by avidin may reduce the flux as intended, but the calcium complexation by the same protein may facilitate the ion transfer. This is supported by the observation of improved calcium ion transport in the presence of an outermost layer of poly(acrylic acid) layer on the surface of a calcium-selective membrane.[18] Therefore, the overall effect of the protein layer for calcium ion transfer is difficult to predict. It may be part of the reason why it's difficult for biotin immobilized polyurethane calcium-selective membrane to show a clear response to the presence of streptavidin in earlier work by Pretsch *et al.*.[21]

The sodium ion blocking effect induced by protein coverage may be used to quantitatively determine the concentration of protein present in the sample, as illustrated in Figure 4. For each point, the potential was first recorded before contact with avidin solution, and the electrode was washed with buffer then immersed into the avidin solution for 12 min. The electrode was subsequently washed again with buffer to remove excess protein and the potential was recorded again in the original protein-free sample. The reaction time of protein and membrane was chosen to be 12 min, which was determined by the potential monitoring of sequential conditioning of membrane in 1 mL of 0.1 mg/mL avidin solution with 2 min increments when

the measuring sample contained 1 mM sodium chloride and 10 mM magnesium nitrate in Tris buffer. It takes about 10 min for the potential to become stable, and an incubation time of 12 min was selected for further work. Figure 4 demonstrates the gradual potential drop upon increased protein concentration with a measuring range of about 1.5–10 μg·mL$^{-1}$.

In this approach, the sensitivity is dependent on the surface coverage of the protein molecules. Theoretically, reducing the surface area and achieving a more effective hemispherical diffusion pattern may lower the detection limit and make the measurement more sensitive. Nanopore membranes are utilized in resistive pulse sensors for monitoring proteins and DNA,[24, 29] and potentiometric protein detection has been demonstrated in combination with gold plated nanopore membranes with modified inner walls exhibiting protein affinity.[14] Here, a two-layer membrane was explored for sensing purposes. The top layer was a poly(vinylpyrrolidone) (PVP) wetted hydrophilic track-etched polycarbonate nanopore membrane without any sensing component while the bottom layer was the biotin modified sodium-selective membrane described above. The purpose of this assembly was to reduce the effective membrane area to the net pore area, while keeping the recognition chemistry unchanged relative to the approach described above.

The electrochemical response of membrane modified electrodes has been studied at metal/electrolyte as well as two immiscible electrolytes interfaces.[27, 28] The electrochemical behavior is usually explained as a microelectrode array, having either an inlaid or recessed surface, depending on how the membrane electrode is assembled.[27, 28] The most common technique to characterize such electrodes is cyclic voltammetry, and the relationship between the limiting current and the electrode geometry has been derived. If the membrane electrode behaves as an inlaid microelectrode array, the limiting current can be described as:[28]

$$I_{\text{lim}} = 4\rho AzFDcr \tag{1}$$

While for a recessed microelectrode array, the limiting current will follow:[28]

$$I_{\text{lim}} = 4\rho AzFDcr\frac{\pi r}{\pi r + 4L} \tag{2}$$

Where ρ is the porosity of the nanopore membrane (pore/cm$^2$), A is the entire membrane area, and z, D, c are the charge, the diffusion coefficient and the bulk concentration of transferring ions, respectively; r and L represent the average pore radius and the recess length, as shown in Scheme 1.[27, 28] According to the two equations above, a linear relationship is expected between the limiting current and the aqueous bulk concentration of active ions if the ion diffusion in the aqueous sample is the rate-limiting step.

Figure 5A shows cyclic voltammograms of calcium-selective membranes with and without nanopore membrane cover in a sample containing 30 μM calcium chloride and 1 mM sodium chloride at a scan rate of 10 mV/s. Without nanopore membrane, the negative potential induced calcium ion transport in direction of the membrane gives a current peak at about −0.12 V, indicating calcium ion depletion at the membrane surface, while the peak for the reverse scan at about 0 V may denote the calcium ion transferring from the membrane back to the aqueous sample. A second peak at −0.28 V may originate from the transport of background sodium ions, since this peak also appears in the voltammogram for sodium chloride background alone (data not shown).

When the sensing membrane is covered with the nanopore membrane, the peaks disappear and the limiting current for calcium mass transport is about 0.39 μA, likely indicating the radial

diffusion kinetics at the opening of the pores. The calculated relationship between limiting currents and calcium concentrations for inlaid and recessed microelectrode arrays are illustrated in Figure 5B, together with the experimental results. In the calculation, the values of ρ, r and L are as provided by the membrane manufacturer, and D is chosen as $10^{-5}$ cm/s$^2$, a typical diffusion coefficient for small ions in aqueous solution. The experimental results correspond well to the theoretical predictions for recessed electrodes for concentrations lower than 50 μM. A flattening of the current is observed for higher concentrations, suggesting that the limiting step shifts to the diffusion in the membrane phase.

It is also possible to characterize the nanopore membrane electrodes in pulsed chronopotentiometric measurements. The selectivity of such pulstrodes can be switched from primary ions to more lipophilic electrolyte if the applied current density is sufficiently high, because the current controlled ion flux can be set to overwhelm the mass transport of ionophore.[20] Since it is the current density that determines the ion flux, the smaller active electrode area may require less current to complex all available ionophore. Figure 6 presents the comparison of ionophore depletion experiments for sodium-selective electrodes in 10 mM sodium chloride solution with and without nanopore membrane coverage. The regular membrane shows a total ionophore depletion at about 36 μA while for nanopore modified membrane, the saturation of ionophore occurs at about 3 μA. The ratio of the saturation currents (about 12) is smaller than the ratio of effective membrane areas (about 33), likely due to the multi-dimensional diffusion kinetics in the organic phase for nanopore membranes.

The same experiment as in Figure 4 was conducted to measure the amount of avidin deposited on a nanopore modified biotin linked membrane and the result is shown in Figure 7. The measuring range for avidin shifts to significantly lower concentration compared with the regular biotin linked membrane, from about 1.5–10 μg·mL$^{-1}$ to 0.1–1 μg·mL$^{-1}$. The magnitude of this shift correlates well with the ratio of the effective membrane area, suggesting an improved detection limit owing to the nanopore membrane modification and a low level of non-specific protein adsorption on the nanopore membrane surface. In this comparison, the potential was sampled at the end of a zero current pulse immediately after the applied current pulse[37] in order to eliminate the influence of nanopore membrane resistance on the sensor response. Note that compared with Figure 4 (without nanopore membrane), the total potential drop for avidin sensing is decreased significantly with the nanopore membrane. The reason for this is not completely clear, but may be related to an incomplete surface coverage of avidin at high concentrations, which may be due to the constriction afforded by the nanopore membrane or a an imperfect sealing between the nanopore membrane and the underlying ion sensing polymer membrane.

## Conclusions

A pulsed chronopotentiometric ion sensor (pulstrode) has been applied to explore the concept of ion channel mimetic sensing on polymeric membranes, using an avidin-biotin interaction as a model system. The bio-affinity between the protein in the sample and the biotin group covalently attached to the membrane results in the accumulation of protein on the sensor surface that could not be washed away. Using membranes that are selective to sodium ions as marker ions in this ion channel mimetic approach, a large potential drop in the so-called super-Nernstian step of the chronopotentiometric calibration curve was observed. The response is attributed to the partial blocking of the instrumentally controlled ion flux in the vicinity of the membrane. The potential drop can be employed to measure the protein concentration and the specificity of the protein-sensor interaction is demonstrated by the comparison of impedance spectra of biotinylated and un-biotinylated ion-selective membranes. The lower detection limit for protein detection is improved by assembling a hydrophilic nanoporous thin film on top of the sensor surface in order to reduce the effective membrane surface area that is available to

protein loading. Such nanopore membrane modified electrodes are characterized by pulsed chronopotentiometry and cyclic voltammetry, supporting the recessed nanoelectrode array model. The protein measuring range upon nanopore membrane modification is shifted to lower concentration by more than one order of magnitude, and this shift is in accordance with the change in active surface area. The lower detection limit for protein sensing may be further reduced by decreasing pore density and size of the nanopore membrane. The sensing strategy explored here may be a promising platform for bioaffinity sensing, such as the sensing based on antibody-antigen and sugar-lectin interactions. The measuring sensitivity could be expected to increase if the target biomolecules have higher charge densities. A key challenge lies in the non-specific adsorption of the sensing polymer membrane, which might be a bottleneck in real applications when complex samples may foul the membrane surface. This problem may be diminished by using polymers with lower non-specific adsorption properties such as cellulose triacetate[32] or adequate surface pretreatment.[38, 39]

## Acknowledgements

We thank Dr. Garth Simpon for the experiment discussion and the National Institutes of Health (EB002189 and GM07178) for financial support.

## References

1. Limoges B, Marchal D, Mavre F, Saveant J-M. J. Am. Chem. Soc 2008;130:7276–7285. [PubMed: 18491854]
2. Numnuam A, Chumbimuni-Torres KY, Xiang Y, Bash R, Thavarungkul P, Kanatharana P, Pretsch E, Wang J, Bakker E. Anal. Chem 2008;80:707–712. [PubMed: 18184015]
3. Numnuam A, Chumbimuni-Torres KY, Xiang Y, Bash R, Thavarungkul P, Kanatharana P, Pretsch E, Wang J, Bakker E. J. Am. Chem. Soc 2008;130:410–411. [PubMed: 18092783]
4. Patolsky F, Lichtenstein A, Willner I. Angew. Chem., Int. Ed 2000;39:940–943.
5. Lee KS, Kim T-H, Shin M-C, Lee W-Y, Park J-K. Anal. Chim. Acta 1999;380:17–26.
6. Umezawa Y, Aoki H. Anal. Chem 2004;76:320A–326A.
7. Odashima K, Kotato M, Sugawara M, Umezawa Y. Anal. Chem 1993;65:927–936.
8. Sugawara M, Kojima K, Sazawa H, Umezawa Y. Anal. Chem 1987;59:2842–2846. [PubMed: 2449097]
9. Gadzekpo VPY, Buhlmann P, Xiao KP, Aoki H, Umezawa Y. Anal. Chim. Acta 2000;411:163–173.
10. Zhan D, Xiao Y, Yuan Y, He Y, Wu B, Shao Y. J. Electroanal. Chem 2003;553:43–48.
11. Ye Q, Vincze A, Horvai G, Leermakers FAM. Electrochim. Acta 1998;44:125–132.
12. Strutwolf J, Manzanares JA, Williams DE. Electrochem. Commun 1999;1:139–144.
13. Martins MC, Pereira CM, Santos HA, Dabirian R, Silva F, Garcia-Morales V, Manzanares JA. J. Electroanal. Chem 2007;599:367–375.
14. Gyurcsanyi RE, Vigassy T, Pretsch E. Chem. Commun 2003:2560–2561.
15. Muslinkina L, Pretsch E. Chem. Commun 2004:1218–1219.
16. De Marco R, Ng A, Panduwinata D. Electroanalysis 2008;20:313–317.
17. Xu Y, De Marco R, Shvarev A, Bakker E. Chem. Commun 2005:3074–3076.
18. Xu Y, Xu C, Shvarev A, Becker T, De Marco R, Bakker E. Anal. Chem 2007;79:7154–7160. [PubMed: 17711298]
19. Makarychev-Mikhailov S, Shvarev A, Bakker E. Anal. Chem 2006;78:2744–2751. [PubMed: 16615788]
20. Shvarev A, Bakker E. Anal. Chem 2003;75:4541–4550. [PubMed: 14632062]
21. Reichmuth P, Sigrist H, Badertscher M, Morf WE, de Rooij NF, Pretsch E. Bioconjugate Chem 2002;13:90–96.
22. Bayley H, Martin CR. Chem. Rev 2000;100:2575–2594. [PubMed: 11749296]
23. Harrell CC, Lee SB, Martin CR. Anal. Chem 2003;75:6861–6867. [PubMed: 14670046]

24. Harrell CC, Choi Y, Horne LP, Baker LA, Siwy ZS, Martin CR. Langmuir 2006;22:10837–10843. [PubMed: 17129068]
25. Ervin EN, White HS, Baker LA. Anal. Chem 2005;77:5564–5569. [PubMed: 16131066]
26. Ito T, Audi AA, Dible GP. Anal. Chem 2006;78:7048–7053. [PubMed: 17007534]
27. Kralj B, Dryfe RAW. Phys. Chem. Chem. Phys 2001;3:5274–5282.
28. Kralj B, Dryfe RAW. Phys. Chem. Chem. Phys 2001;3:3156–3164.
29. Siwy Z, Trofin L, Kohli P, Baker LA, Trautmann C, Martin CR. J. Am. Chem. Soc 2005;127:5000–5001. [PubMed: 15810817]
30. Qin Y, Peper S, Radu A, Ceresa A, Bakker E. Anal. Chem 2003;75:3038–3045. [PubMed: 12964748]
31. Shvarev A, Bakker E. Talanta 2004;63:195–200. [PubMed: 18969419]
32. Cha GS, Meyerhoff ME. Talanta 1989;36:271–278. [PubMed: 18964700]
33. Liu D, Meyerhoff ME, Goldberg HD, Brown RB. Anal. Chim. Acta 1993;274:37–46.
34. Walcerz I, Glb S, Koncki R. Anal. Chem. Acta 1998;369:129–137.
35. Tinkilic N, Cubuk O, Isildak I. Anal. Chem. Acta 2002;452:29–34.
36. Horvai G, Graf E, Toth K, Pungor E, Buck RP. Anal. Chem 1986;58:2735–2740.
37. Makarychev-Mikhailov S, Shvarev A, Bakker E. J. Am. Chem. Soc 2004;126:10548–10549. [PubMed: 15327306]
38. Zhang M, Ferrari M. Biotechnol. Bioeng 1997;56:618–625. [PubMed: 18642333]
39. Uchida K, Otsuka H, Kaneko M, Kataoka K, Nagasaki Y. Anal. Chem 2005;77:1075–1080. [PubMed: 15858988]

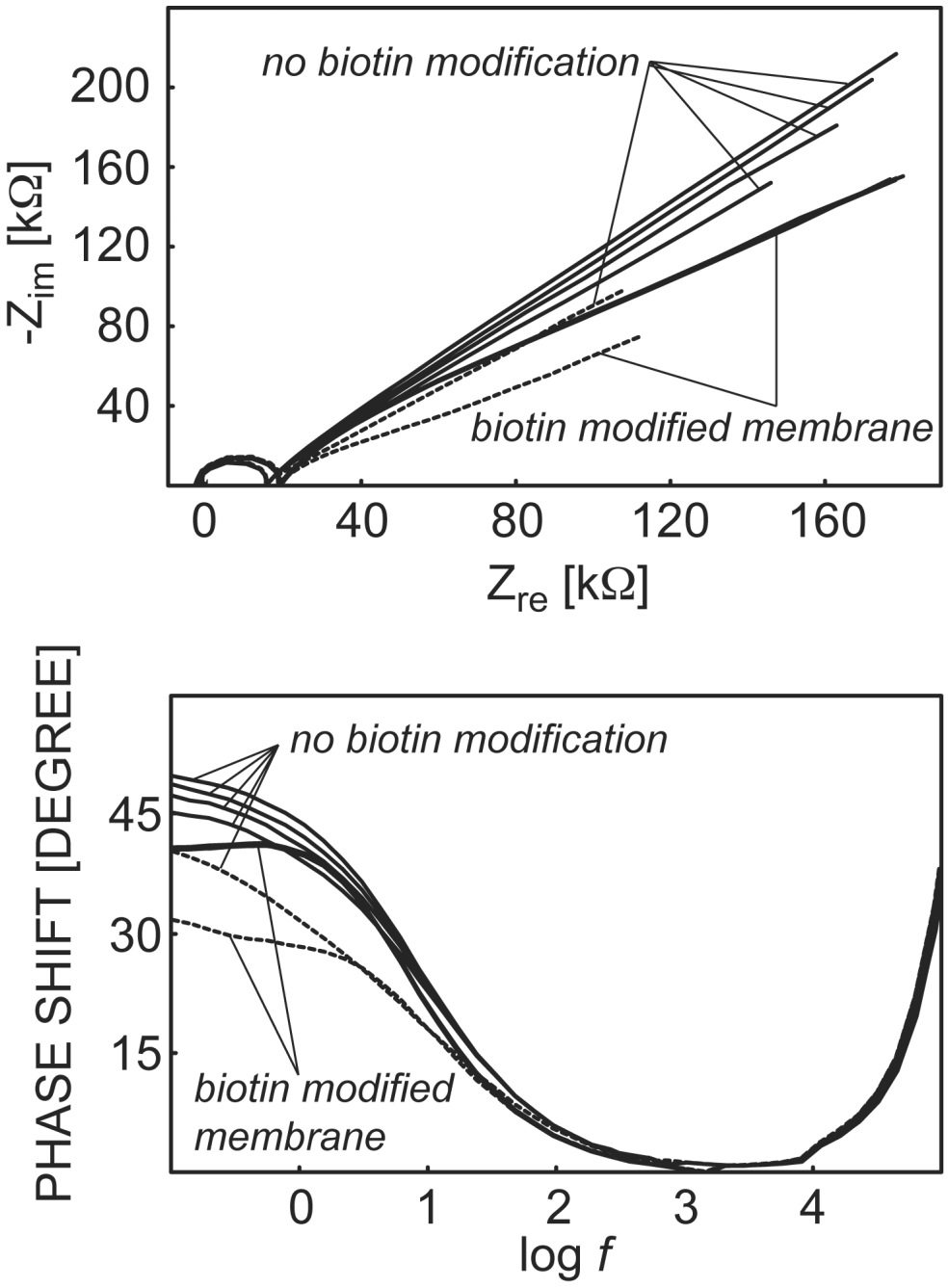


**Figure 1.**
Comparison of electrochemical impedance (A) Nyquist plots and (B) Bode plots for sodium-selective membranes in 10 mM magnesium nitrate and 1 mM Tris-$HNO_3$ buffer (pH 7.4) before (dashed line) and after (solid line) avidin treatment and multiple washing steps.

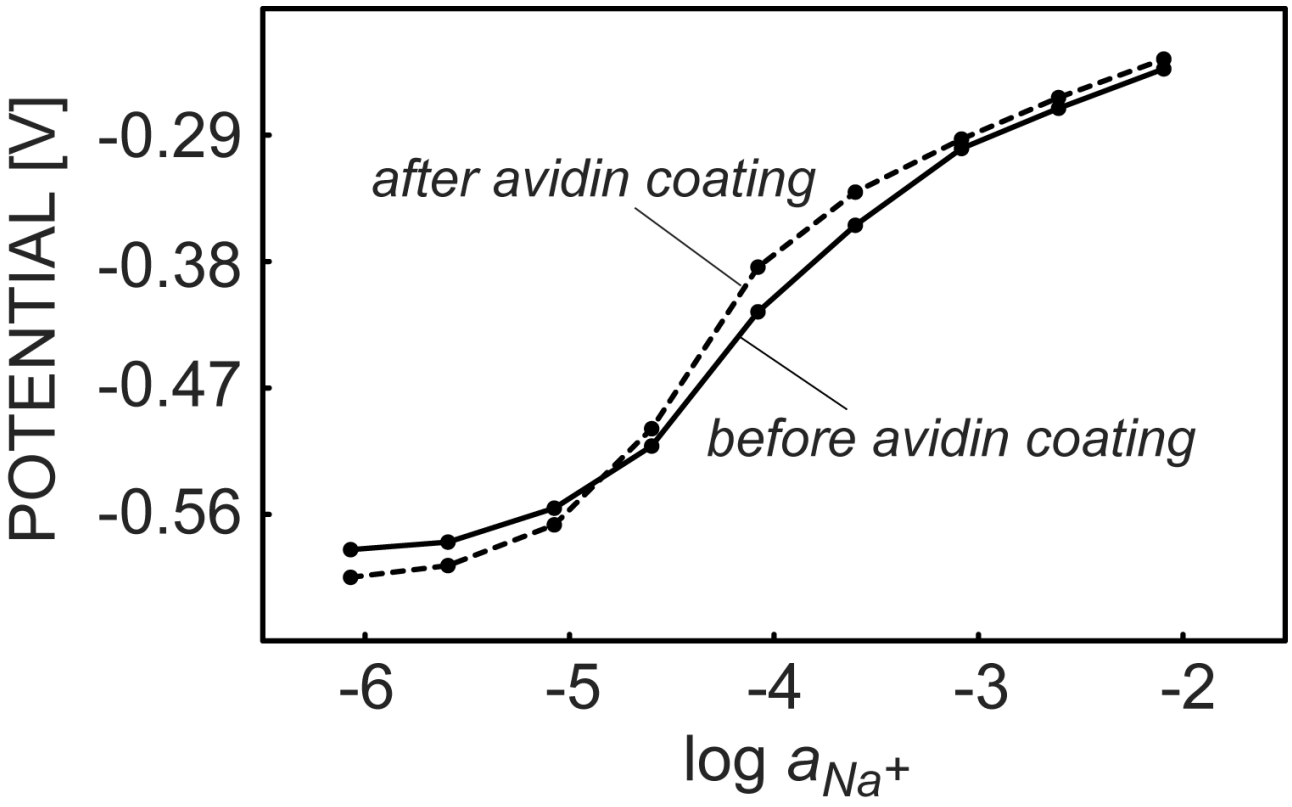


**Figure 2.**
Pulsed chronopotentiometric sodium response of a sodium-selective membrane without biotin attachment sampled at the end of a 0.5 s cathodic current pulse (current density is 0.4 μA/mm$^2$), in a background solution of 10 mM magnesium nitrate and 1 mM Tris-$HNO_3$ buffer (pH 7.4).

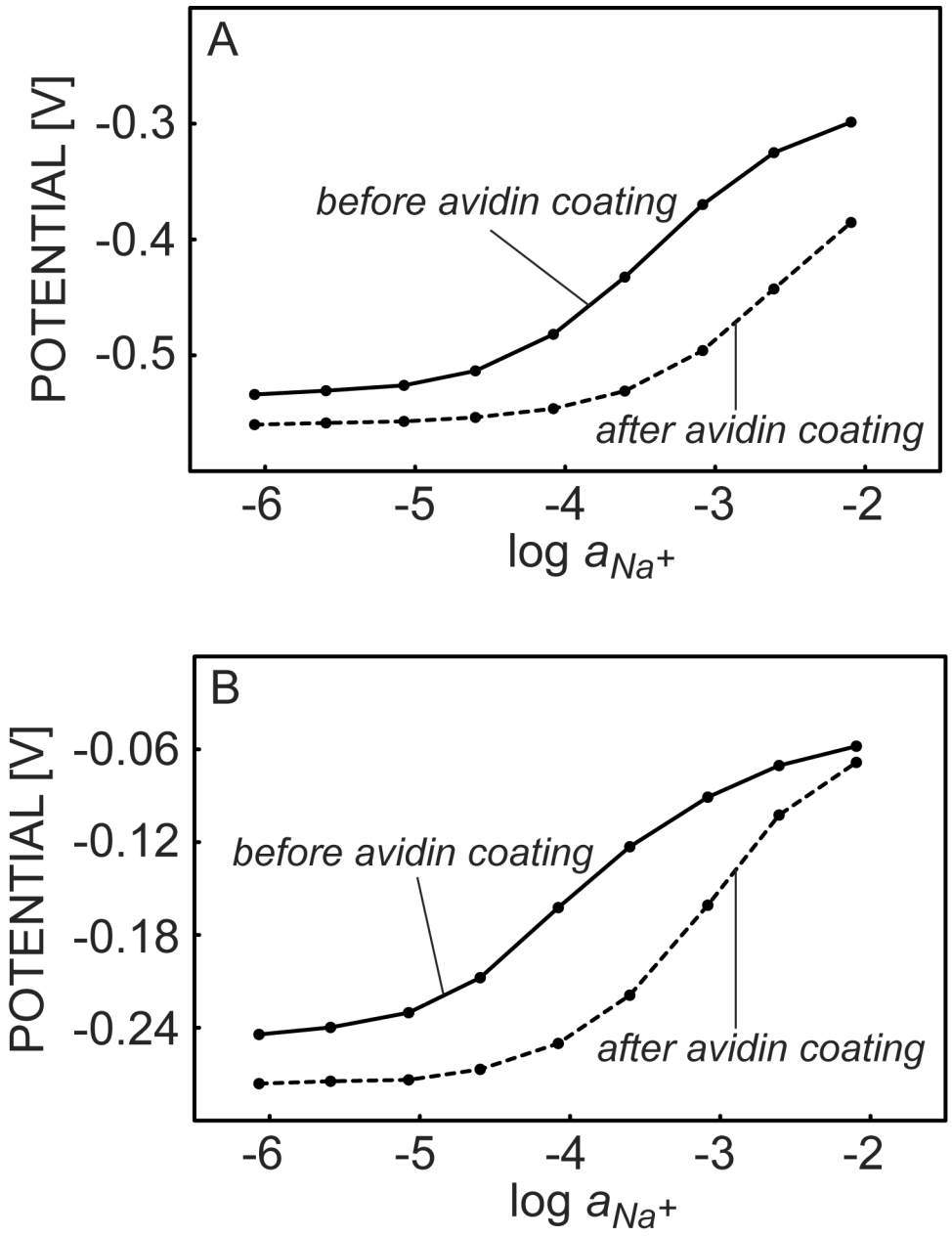


**Figure 3.**

Pulsed chronopotentiometric sodium response of a sodium-selective biotinylated membrane, sampled at the end of (A) a 0.5 s cathodic current pulse (current density is 0.4 μA/mm$^2$) and (B) a 0.5 s zero current pulse imposed immediately after the cathodic current pulse. Background solution as in Figure 2.

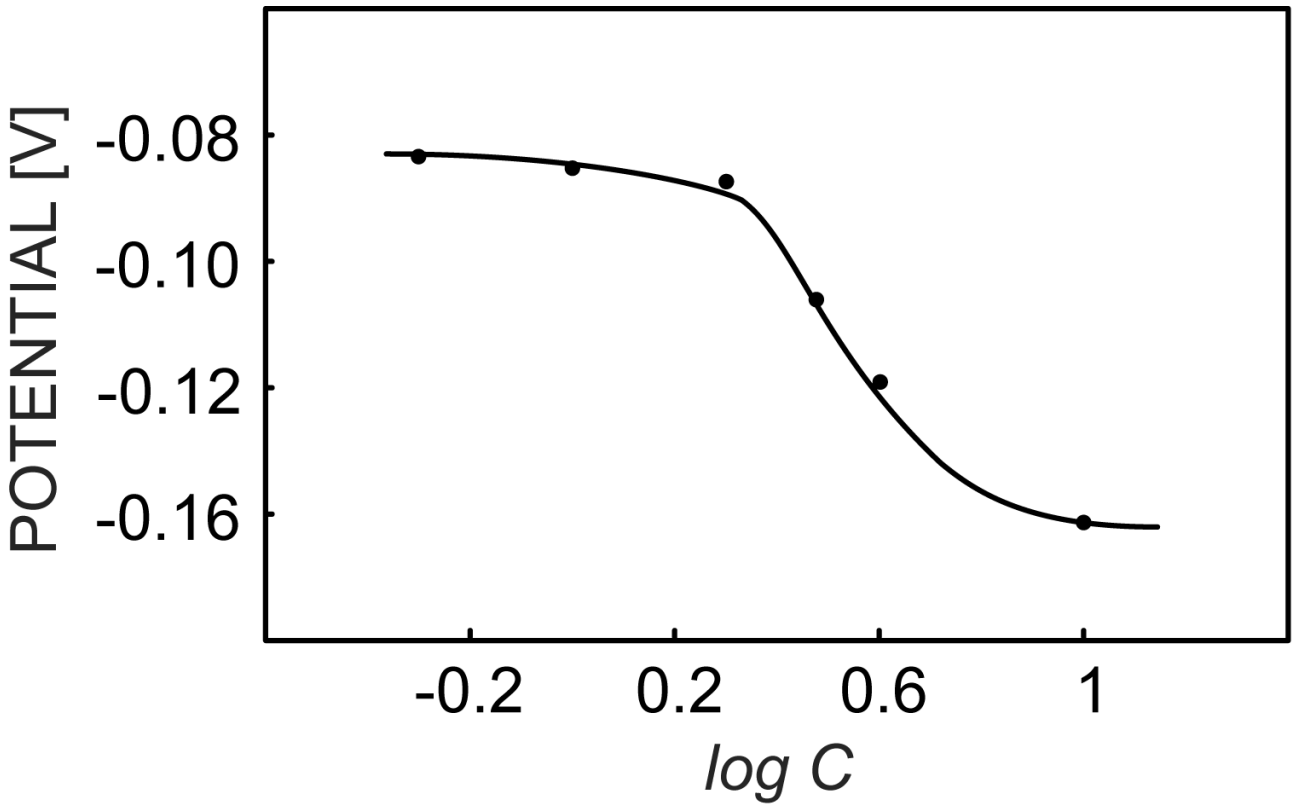


**Figure 4.**
Pulsed chronopotentiometric response of a sodium-selective biotinylated membrane, sampled at the end of a 0.5 s zero current pulse, to varying concentrations of avidin (in units of $mg \cdot mL^{-1}$). The sample contained 1 mM sodium chloride in an electrolyte background as in Figure 2.

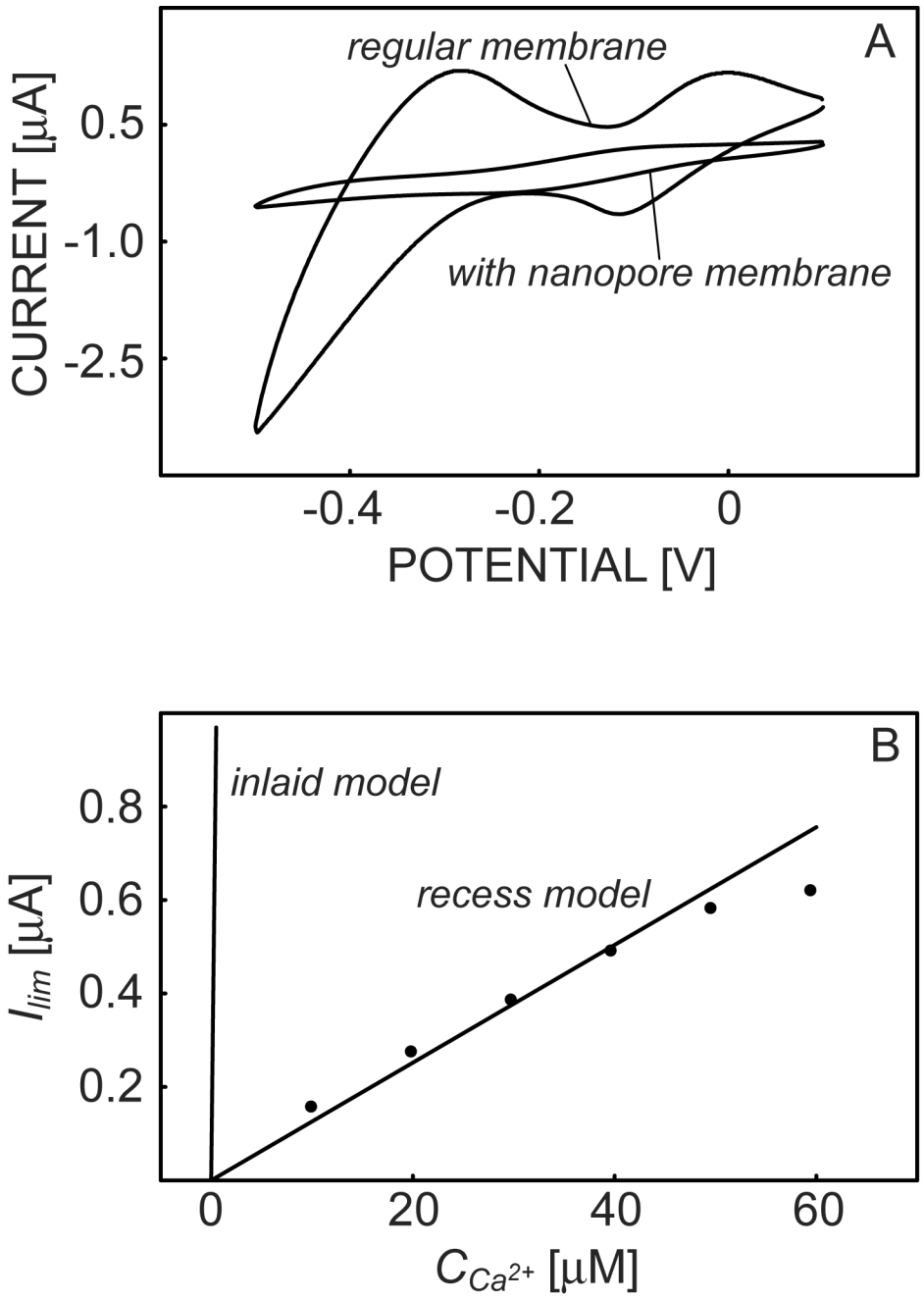


**Figure 5.**

Cyclic voltammetric characterization of nanopore membrane electrodes. (A) Voltammograms of calcium-selective electrodes with and without nanopore membrane modification when the sample contained 30 µM calcium chloride and 1 mM sodium chloride. (B) Calculated and experimental limiting currents at varying calcium ion concentrations. The background solution contained 1 mM sodium chloride.

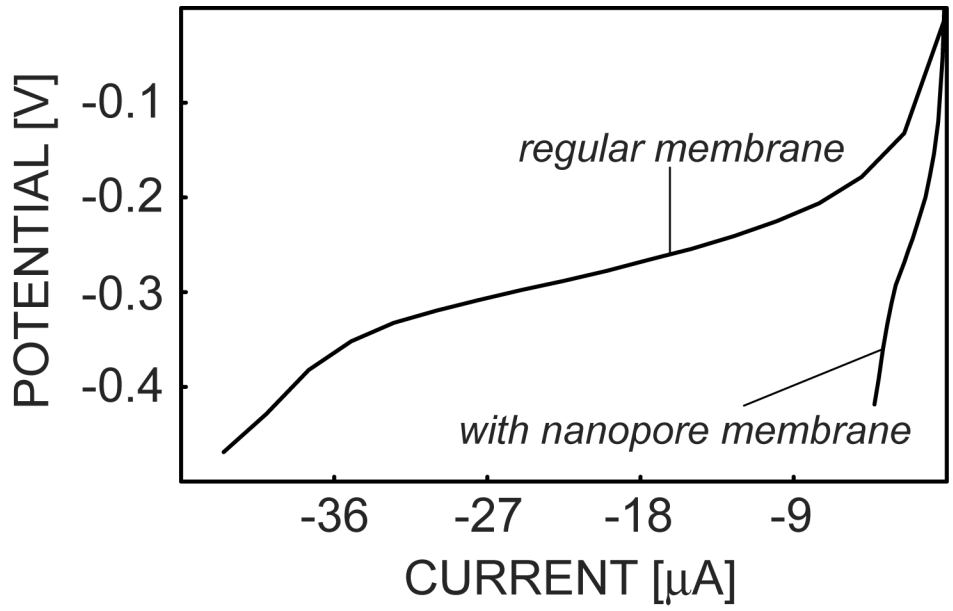


**Figure 6.**
Pulsed chronopotentiometric response of sodium ionophore depletion measurements with and without nanopore membrane modification. The sample contained 10 mM sodium chloride.

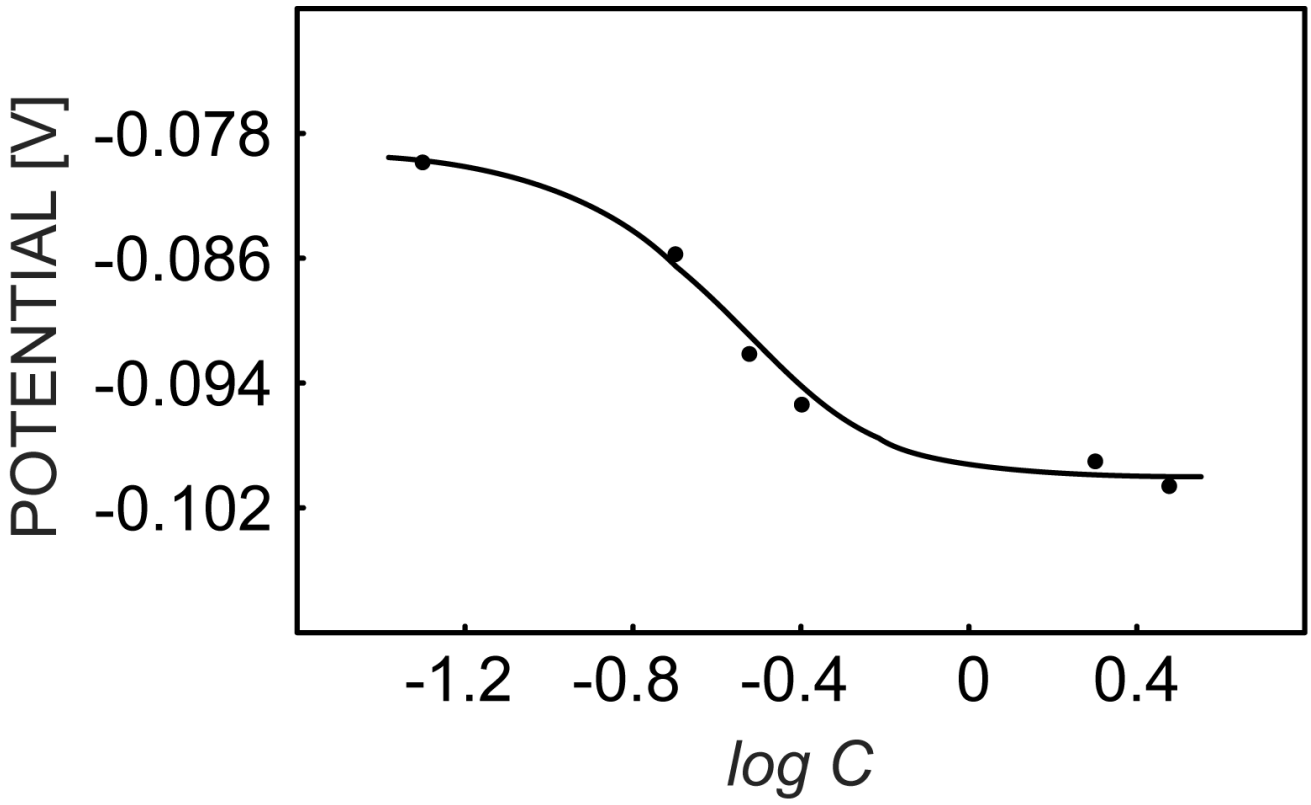


**Figure 7.**
Pulsed chronopotentiometric response of a sodium-selective biotinylated membrane covered with a hydrophilic nanopore membrane, sampled at the end of a 0.5 s zero current pulse, to varying concentrations of avidin (in units of $mg \cdot mL^{-1}$). The measuring sample contained 10 mM sodium chloride, 10 mM magnesium nitrate and 1 mM Tris-$HNO_3$ buffer (pH 7.4).

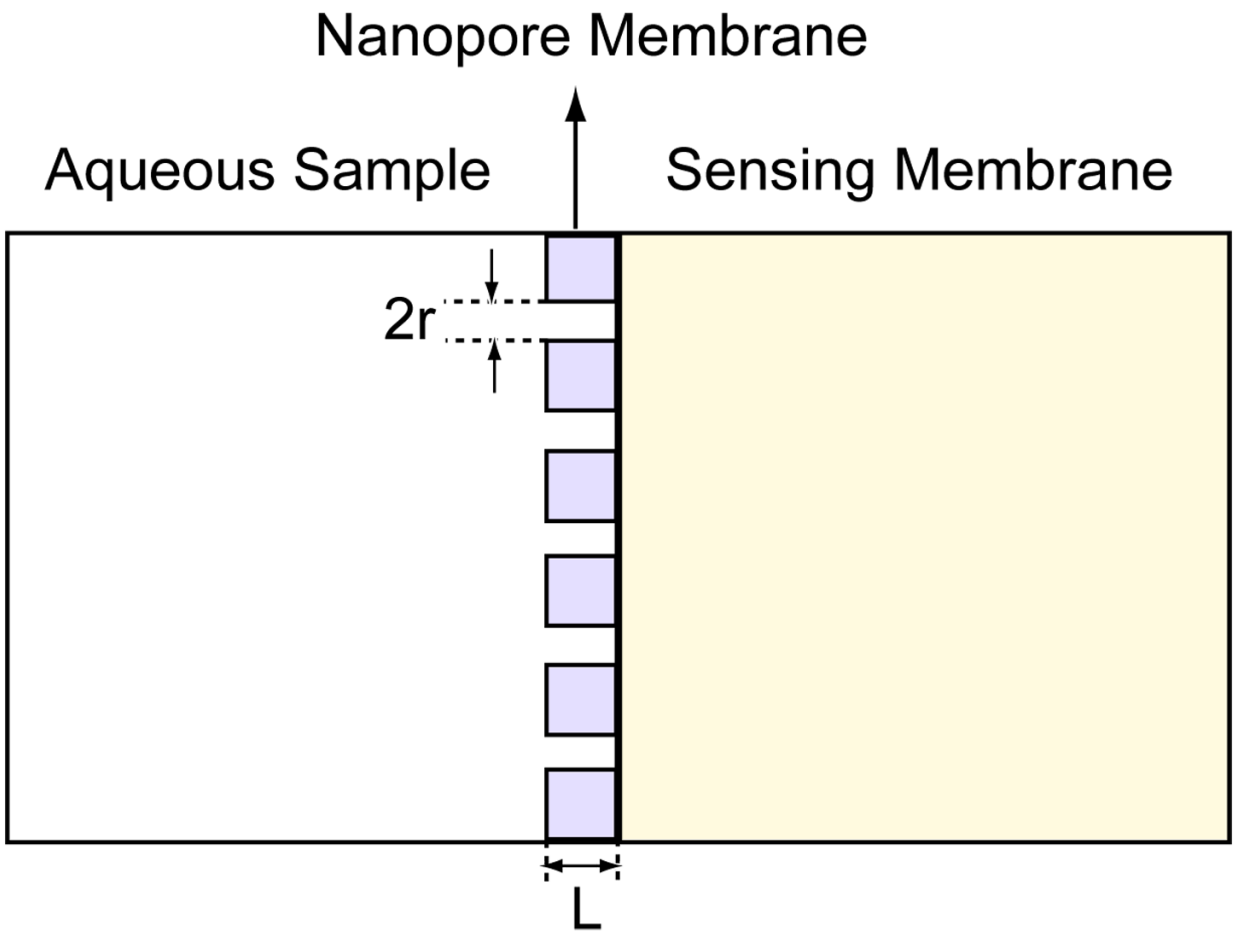


**Scheme 1.**
Schematic configuration of the nanopore membrane modified aqueous/membrane interface.